Acta Oceanol. Sin., 2018, Vol. 37, No. 3, P. 111–116
DOI: 10.1007/s13131-018-1204-6
http://www.hyxb.org.cn
E-mail: hyxbe@263.net

A routine operational backscattering coefficient regrouping algorithm for a HY-2A scatterometer

ZOU Juhong[1, 2*], LIN Mingsen[2], ZOU Bin[2], GUO Maohua[2], ZHANG Yi[1, 2]

[1] Key Laboratory of Space Ocean Remote Sensing and Application, State Oceanic Administration, Beijing 100081, China

[2] National Satellite Ocean Application Sevice, State Oceanic Administration, Beijing 100081, China

Received 24 March 2017; accepted 10 August 2017

Abstract

The routine operational sigma0 regrouping method is proposed for a HY-2A scatterometer (HSCAT) that maps time-ordered sigma0s and related parameters into a subtrack aligned grid of wind vector cells (WVCs). The regrouping method consists of two critical steps: ground grid generation and sigma0 resampling. The HSCAT uses subtrack swath coordinates, in which the nadir track of the satellite represents the center and the designated positions are specified in terms of a pair of along-track and cross-track coordinates. To calculate the subtrack coordinates for each sigma0, a "triangle marking" resampling method is developed. Three points, including the point of intersection, the center of a pulse footprint, and the origin of the subtrack coordinate system, form a right triangle; the length of the two right-angled sides is used to represent the cross-track and the along-track coordinates in the subtrack coordinate system. In addition, a nadir point interpolation correction is used to ensure the operation of the regrouping algorithm when the nadir point positional information is missing. To illustrate the ability of the proposed regrouping algorithm, the distribution of the WVC positions and wind vector retrieval results are analyzed, which show that the proposed regrouping algorithm meets the requirements for high-quality sea surface wind field retrieval.

Key words: regrouping, HY-2A scatterometer, backscattering coefficient

Citation: Zou Juhong, Lin Mingsen, Zou Bin, Guo Maohua, Zhang Yi. 2018. A routine operational backscattering coefficient regrouping algorithm for a HY-2A scatterometer. Acta Oceanologica Sinica, 37(3): 111–116, doi: 10.1007/s13131-018-1204-6

1 Introduction

Satellite scatterometers have become a primary tool for global sea surface wind vector (SSWV) observations. A scatterometer can indirectly measure the SSWV by measuring the backscattering coefficient of the sea surface after it is modulated by the sea surface wind field. Typically, acquiring SSWV data from scatterometer measurements require several processing steps, including geo-location, radiometric calibration, regrouping, wind vector retrieval and ambiguity removal. Since the backscattering coefficient exhibits dual-cosine distribution characteristics of the wind vector, an accurate retrieval of the wind vector requires the observed backscattering coefficients to possess no less than three azimuth/incident angles (Naderi et al., 1991). To satisfy this requirement, the scatterometer's measurement geometry has to be well designed and the scatterometer's observed results must be resampled to the wind vector cells (WVCs) for a specific grid. The wind vector retrieval is generally performed based on each WVC, which means that the acquired wind vector is an average value of the wind vectors at this scale. Regrouping refers to the process of resampling the measurements that are stored based on the observational time sequence of the WVC so that the subsequent wind vector retrieval can be conducted. Since the regrouping results can directly affect the accuracy of the final measurement, researchers worldwide have carefully designed a number of regrouping methods based on the scatterometer's observation characteristics.

The Europe remote-sensing satellite (ERS) scatterometer has a grid pattern for the WVC and the measurements are interpolated into a 25 km×25 km grid network. The position of the central node of the swath is in the intersection of the mid antenna's line of sight to the earth (defined by GEM6). The other nodes are located along the intersection of the plane defined by the center of the earth, the satellite, and the mid antennae's line of sight every 25 km in both directions. This is repeated for every four measurement blocks, which corresponds to 3 763.36 ms or roughly 25 km on the ground. Since the Earth's surface is tabular, the grid lines connecting these nodes are not strictly parallel to each other (Lecomte, 1998).

Similar as in the ERS scatterometer, a two-dimensional Hamming window centered at every swath's grid node position is used to perform the sigma0s regrouping in an advanced scatterometer (ASCAT). The width of the window is defined by the principal cut in the along- and across-track directions as the distance to the center of the spatial filter when it reaches 50% of the peak value. To deal with winds closer to the coast, a resampling step with a circular top-hat filter instead of the two-dimensional Hamming window was explored. A circular top-hat filter window of 15 km diameter is used to generate a wind product for a 12.5 km×12.5 km that takes advantage of the smaller size of the circular top-hat window to allow estimation of the resampled land-

Foundation item: The National High Technology Research and Development Program (863 Program) of China under contract No. 2013BAD13B01; the National Natural Science Foundation of China under contract No. 41576177.
*Corresponding author, E-mail: zoujuhong@mail.nsoas.org.cn

free normalized radar cross-section (NRCS) values closer to the coast (EUMETSAT, 2015; Verhoef et al., 2012; Vogelzang et al., 2011).

To regroup the observation results of QuikSCAT, the Jet Propulsion Laboratory uses the Synder's space-oblique Mercator (SOM) projection, in which the ground grid uses the subtrack as the center and the designated position is denoted by both along- and cross-track coordinates. The SOM projection was first proposed for Landsat data and is suitable for relatively narrow near-circular orbits. This type of projection is generally used for charting and the spherical coordinates are converted to Cartesian coordinates via a Fourier transform. To simplify the calculation, the JPL only converts the angular coordinates (Dunbar et al., 2001).

For the scatterometer subsystem of a multimode microwave remote sensor on board the China's Shenzhou-4 unmanned spacecraft, Zhang et al. (2005) developed a grid with a resolution of 50 km×50 km with eight cells in the cross-track direction, so that at least four independent sigma0 measurements are included in each cell. By regrouping the Shenzhou-4 scatterometer's 40 min measurements into these well-designed grids, the sea surface wind field can be retrieved successfully.

In August 2011, China launched the first routine-operational satellite-borne scatterometer, HY-2A scatterometer (HSCAT) (Zou et al., 2014). This made it necessary to design an appropriate regrouping algorithm based on the HY-2A/SCAT measurement geometry. In this study, a routine operational regrouping algorithm for the HSCAT is introduced. Section 2 introduces the characteristics of the HSCAT sensor and the related L1B-level data product; the proposed regrouping algorithm for the HSCAT is described in Section 3; Section 4 describes results; and the conclusions are presented in Section 5.

2 Brief introduction of HSCAT

The HSCAT is China's first routine operational microwave scatterometer. It is carried on board China's HY-2 satellite, which was launched in August of 2011. HSCAT's main task is the sea surface wind field observation on a global scale. The wind speed measurement range is 4–24 m/s, with an accuracy of 2 m/s (or 10%), while the wind direction measurement range is 0°–360°, with an accuracy of 20°. The HSCAT runs at a frequency of 13.256 GHz and uses a pencil-beam conical scanning mode, i.e., it rotates around the nadir at a constant elevation through a pencil beam and creates a ground coverage swath during the satellite platform's along-track movements. The HSCAT follows two polarization modes, VV and HH. During the satellite platform's movements, the HSCAT makes multiple measurements for a same resolution cell from different incident angles, so that the 180° wind direction ambiguities can be removed. The internal beam follows an HH polarization with a 41° incident angle, a 23 km×31 km footprint, and a swath width of 1 350 km. The external beam follows a VV polarization with a 48° incident angle, a 25 km×38 km footprint, and a swath width of 1 700 km (Stoffelen et al., 2001).

HSCAT data products can be classified into several levels, including L1B, L2A, L2B and L3. L1B data are stored in the time sequence of the telemetry frames and are used as the input data in this study. Each L1B data file contains the data observed by the HSCAT during one entire revolution. Each telemetry frame contains the observation time, the longitude and latitude of the corresponding subtrack point, and the measurement data from 96 scatterometer pulses. The pulse repetition frequency (PRF) is 181 Hz and the interval of each frame is approximately 0.54 s, which means that a set of telemetry frame package data is acquired every 0.54 s. The data measured by each pulse include the backscattering coefficient, the geographic position of each pulse footprint, and the parameters used to describe the quality and uncertainty of the measurement data.

3 Regrouping algorithm for HSCAT

Regrouping aims at resampling the sigma0 and related parameters that are stored in the observation sequence to the grid aligned with the subtrack of the WVC. The size of the WVC has to first satisfy the resolution requirements in applications such as numerical weather forecasts. In addition, at least three measurements with different azimuth or incidence angles have to be included in a single WVC, so that the subsequent wind vector retrieval process can be performed adequately. Therefore, we need to design the grid of the WVC carefully and resample each sigma0 and the related parameters.

3.1 *Generation of ground grid*

To simplify the calculations, a convenient swath coordinate system was employed in the HSCAT, in which the nadir track of the satellite is used as the center and the designated positions are denoted by a pair of along- and cross-track coordinates. As shown in Fig. 1, the grid in this swath coordinate system has a resolution of 25 km×25 km and each cell of the grid corresponds to a WVC. The coordinate system's origin is set at the boundary of the HSCAT orbit and corresponds to a location at the southernmost latitude of the satellite's orbit. Since the HSCAT has a fairly narrow swath, it is acceptable to neglect the longitudinal compression on the swath's edge. This model can be regarded as a strictly rectangular network for simplification of the calculations.

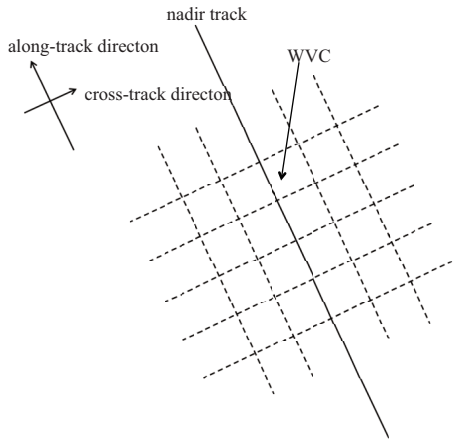

Fig. 1. Illustration of the WVC and the related coordinate system.

3.2 *Resampling of observed results*

The resampling algorithm maps the time-ordered sigma0s and the related parameters into the subtrack aligned grid of the WVCs. In this study, the egg-shaped sigma0s are aggregated into the swath grids. If the center of a sigma0 footprint falls within the WVC, the sigma0s and the related parameters are grouped into the WVC; the location of each sigma0 can be described in terms of a pair of along- and cross-track bin coordinate indices. Therefore, the sigma0 locations that are originally in longitude and latitude coordinates must be accurately transformed to along- and cross-track subtrack swath coordinates. To calculate the subtrack coordinates for the sigma0s, a "triangle marking" res-

ampling method was applied. As shown in Fig. 2, Point P_i corresponds to the position of the footprint's center of the ith pulse and Point S_j corresponds to the position of the jth nadir point, while Point S_1 corresponds to the point at the southernmost latitude of the satellite. A line that runs through Point P_i and is perpendicular to the line of the nadir track intersects that line at Point D. The three points form a right triangle with the Points P_iDS_1. The length of the side P_iD corresponds to the cross-track coordinates in the subtrack coordinate system for Point P_i and the length of the side S_1D corresponds to the along-track coordinates. Once we obtain the position of the Point D, the right triangle P_iDS_1 can be determined, and this can be used to calculate the subtrack coordinates of the sigma0. To obtain the location of the intersection Point D, we use the nadir point position from the L1B data, which provides the geodetic latitude and longitude of the location on the spacecraft's nadir track at the specified time for the first pulse of the frame. The PRF is 181 Hz for the HSCAT and each frame of data contains 96 pulses; therefore, the time interval of each frame is approximately 0.54 s. Considering that the velocity of the HY-2A satellite is approximately 7 km/s, under normal conditions, we can obtain a nadir point position every 3.78 km along the nadir track from L1B data. The position of the nadir point with the shortest distance to Point D was chosen to represent the approximate position of Point D. Considering that the resolution of the WVCs is 25 km, this approximation is acceptable for the purpose of binning HSCAT sigma0s.

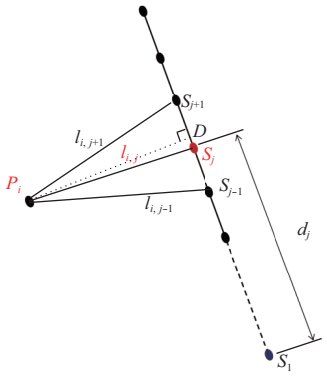

Fig. 2. Geometry for the "triangle marking" resampling method.

By calculating the spherical distance l from P_i to every nadir Point S when the spherical distance l reaches its minimum, the corresponding nadir point can be determined as the point with the shortest distance to Point D, which is Point S_j in Fig. 2. The cross-track coordinate for P_i can be determined by calculating the spherical distance $l_{i,j}$ between point P_i and point S_j, while the along-track coordinate d_j for P_i can be determined by as follows:

$$d_j = \sum_{i=1}^{j} S_i, \tag{1}$$

where S_i corresponds to the spherical distance between the two neighborhood nadir Points S_i and S_{i-1}, which can be calculated by

$$S_i = R\arccos\left[\cos\beta_i \cos\beta_{i-1}\cos(\alpha_i - \alpha_{i-1}) + \sin\beta_i \sin\beta_{i-1}\right], \tag{2}$$

where R corresponds to the radius of the earth; α_i and β_i correspond to the longitude and latitude for the ith nadir point; and α_{i-1} and β_{i-1} correspond to the longitude and latitude for the i–1 nadir point, respectively.

Once the along- and cross-track coordinates are computed, they can be rescaled to the desired swath coordinate system in the along- and cross-track directions to obtain a pair of along- and cross-track bin coordinate indices for P_i.

When S_i is smaller than 12.5 km, which is a half of the resolution of the WVC, it is reasonable to use the position of the nadir point with the shortest distance to Point D to represent the position of Point D. When S_i is close to the resolution of the WVC, this type of approximation will induce a large error. Considering that the HSCAT operates at 24 h a day in a 971 km orbit, it is easily affected by high-energy particles in the universe and thus the electronic components may break down intermittently. In order to ensure a continuous operation, the HSCAT sensor refreshes automatically every day when it passes a specific region. During the resetting interval, the HSCAT cannot effectively acquire measurement data, resulting in an approximate 2 s lack of data such as the nadir positional information. To ensure that the regrouping algorithm works well when there are missing data for the nadir positional information, a nadir point interpolation correction is required.

Since the time interval of a frame is approximately 0.54 s, we assume that the nadir point data are discontinuous and require interpolation if the time interval of the neighboring sub-satellite points t_{i+1}–t_i is greater than 1.08 s. A linear interpolation is applied first to obtaining the time for the interpolated nadir point, as shown as follows:

$$t_p = t_i + n\times 0.54 \quad n = 1, 2, 3, \ldots, ent\left[\frac{t_{i+1} - t_i}{0.54}\right], \tag{3}$$

where t_p corresponds to the time for which the nadir point data require interpolation; and t_i and t_{i+1} correspond to the time for the ith and i+1 nadir points, respectively.

A cubic spline interpolation is used to obtain the longitude and latitude for the interpolated nadir points, as shows in Eqs (4)–(9):

$$\alpha_p = A\alpha_i + B\alpha_{i+1} + C\alpha_i'' + D\alpha_{i+1}'', \tag{4}$$

$$\beta_p = A\beta_i + B\beta_{i+1} + C\beta_i'' + D\beta_{i+1}'', \tag{5}$$

$$A = (t_{i+1} - t_p)/(t_{i+1} - t_i), \tag{6}$$

$$B = (t_p - t_i)/(t_{i+1} - t_i), \tag{7}$$

$$C = \frac{1}{6}(A^3 - A)(t_{i+1} + t_i)^2, \tag{8}$$

$$D = \frac{1}{6}(B^3 - B)(t_{i+1} - t_i)^2, \tag{9}$$

where α_p and β_p correspond to the longitude and latitude for the interpolated nadir point; α_i and β_i correspond to the longitude and latitude for the ith nadir point, which is the nearest nadir point to the interpolated nadir point in the forward direction; α_{i+1} and β_{i+1} correspond to the longitude and latitude for the i+1 nadir point, which is the nearest nadir point to the interpolated nadir point in the backward direction; t_p, t_i and t_{i+1} correspond to the observation time for the interpolated nadir point, the ith point,

and the i+1 nadir point, respectively; α''_{i+1} and α''_{i+1} correspond to the second derivative for the longitudes of the ith point and the i+1 nadir point, which can be calculated by the longitude of the 100 nearest nadir points in the forward and backward directions; and β''_i and β''_{i+1} correspond to the second derivatives for the latitude of the ith point and the i+1 nadir point, which can be calculated by the latitude of the 100 nearest nadir points in the forward and backward directions.

Compared with the data regrouping methods for the QuikSCAT and ERS scatterometers, the proposed "triangle marking" resampling method makes good use of the geodetic information of the nadir point from the L1B data. In addition, the iteration computation in the projection transformation between the earth-located (geodetic) coordinates and the subtrack coordinates is avoided and only simple calculations such as the spherical distance calculation between two point is required, facilitating an easy implementation of the proposed regrouping method for the routine operations. Moreover, by introducing an interpolation correction for the nadir point, the proposed regrouping algorithm operates well when nadir point positional information is missing, which enhances the robustness of the regrouping algorithm.

4 Experimental results

To illustrate the usefulness of the proposed regrouping algorithm, we analyzed the distribution of the WVC positions and the wind vector retrieval results, which are shown in Figs 3 and 4. For comparison, the results before and after the interpolation correction are shown. Figure 3 displays the spatial distribution of the locations of the gravity centers of the WVCs after regrouping. It is evident that the WVC locations are distributed uniformly in most cases except in the nadir region and blank strips along the cross-track direction can be observed (Fig. 3a). Because of the HSCAT's automatic resetting, the distribution of the sub-satellite coordinates was discontinuous, which led to the appearance of cross-track blank strips. Therefore, the proposed regrouping algorithm could not be applied properly in this region, which in turn caused a discontinuous spatial distribution of the along-track grids in these regions. These abnormalities can be eliminated by optimizing the regrouping methods through a nadir track point interpolation, as shown in Fig. 3b. The results show that the WVCs have a more uniform distribution in both the along- and cross-track directions and the cross-track blank strips induced by the discontinuous spatial distribution of the L1B data are eliminated.

The number of independent observation results for the wind vector cells was also analyzed and the statistical results are shown in Fig. 4. The cross-track blank strip was also present (Fig. 4a) but was eliminated by optimizing the regrouping methods through the nadir track point interpolation, as shown in Fig. 4b.

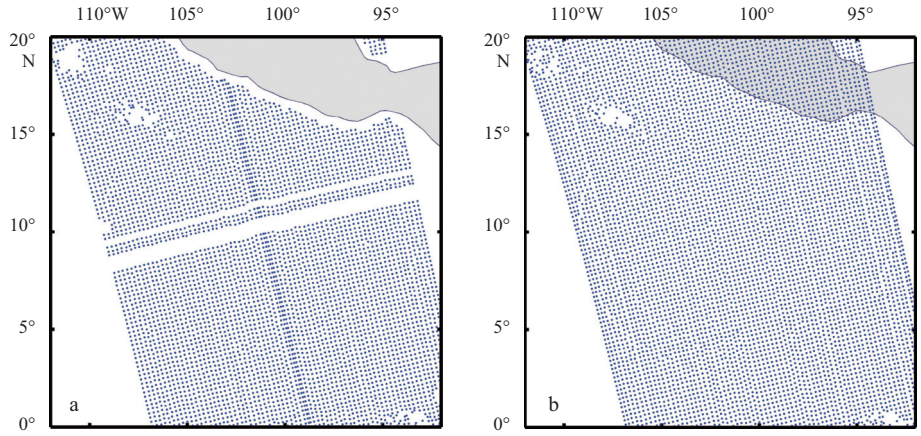

Fig. 3. Distribution of the gravity centers of the WVCs without interpolation (a) and with interpolation (b) (May 30, 2015).

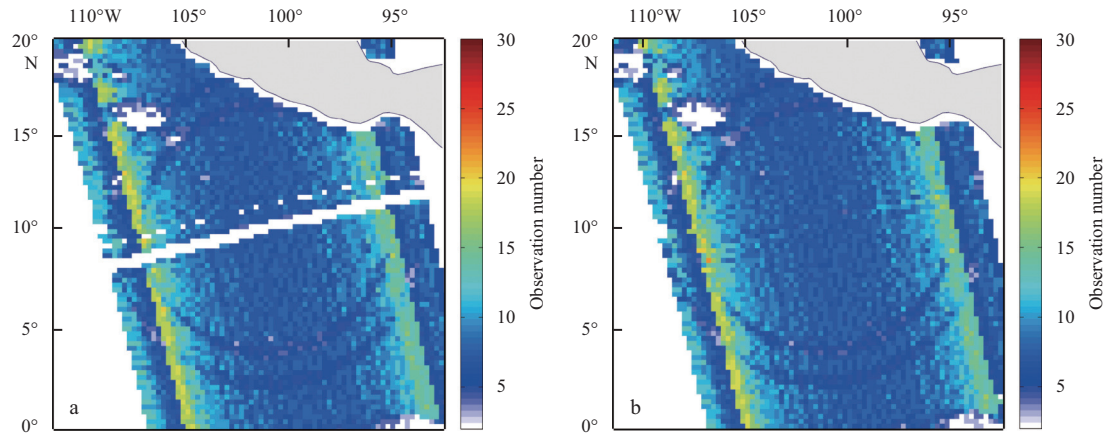

Fig. 4. Distribution of the observation numbers for the wind vectors from different azimuth angles without interpolation (a) and with interpolation (b).

In addition, there were some ring-shaped dark strips centered at the cross-track blank strip, suggesting a lower number of independently observed results in these regions. Since the HSCAT uses a conical scanning mode, the observations during the HSCAT's autonomous resetting period should show a ring-shaped distribution; these ring-shaped dark strips could not be removed by the interpolation algorithm because the HSCAT's automatic resetting was no effective results in these regions.

The ultimate aim of regrouping is to provide data for the wind vector retrieval; therefore, the wind vector retrieval results were also used to evaluate the effectiveness of the proposed regrouping algorithm. In this study, the wind vector was retrieved from the regrouping sigma0s using a multiple solution scheme (MSS) in conjunction with a two-dimensional variational ambiguity removal (2DVAR) method (Stoffelen et al., 2001; Vogelzang, 2007; Vogelzang et al., 2011) (Fig. 5). Figures 5a and b show the wind speed retrieval results, derived from the regrouping results without and with the use of interpolation, respectively. In Fig. 5a, the cross- and along-track blank strips near the nadir track can be observed and they were removed using the interpolation correction. Also, ring-shaped blank strips centered at the nadir track are visible in Figs 5a and b. During the HSCAT's automatic resetting period, no effective results were observed in these regions, resulting in the appearance of the ring-shaped blank strips. This, in turn, caused the observed results in these regions to not reach the minimum number of different azimuth or incidence angles for the wind vector retrieval, i.e., the wind vector could not be accurately retrieved in these regions.

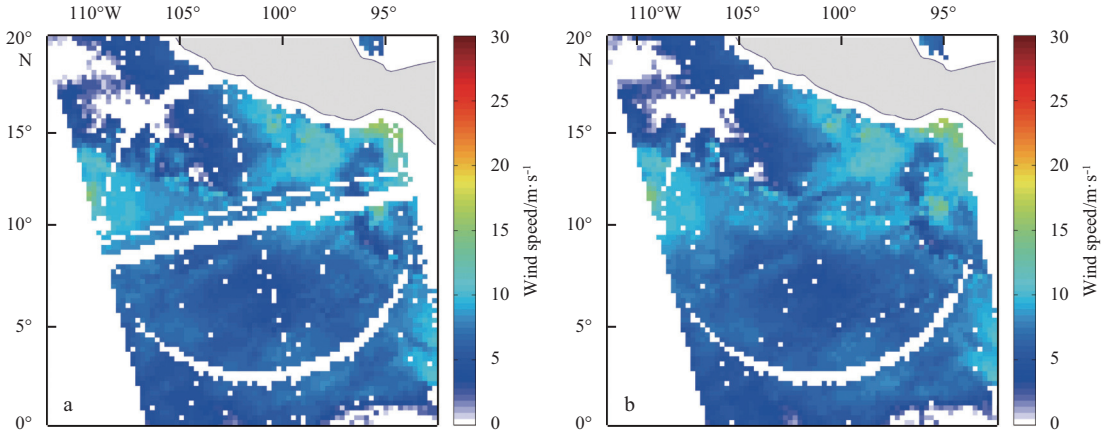

Fig. 5. Retrieval results of wind speed on May 30, 2015 without interpolation (a) and with interpolation (b).

To further validate the regrouping algorithm, the wind vector retrieval results were validated using 10 min averaged SSWV *in situ* buoy observation data, which were provided by the National Data Buoy Center (NDBC). The buoys' wind data were adjusted to a 10 m height. The wind vector retrieval results were matched with the *in situ* data and the *in situ* and fused SSWV data were acquired within 10 min of each other. The geographic location of the measured data was regarded as the center of the WVC and the data were from the SSWV product within a spatial range of 25 km. The matched *in situ* and remote-sensing observation data were limited to points further than 50 km from land and within a reasonable wind speed range. For the period of January 1–31, 2013, 409 sets of retrieved wind data and buoy observations were matched and the results of the statistical analysis are shown in Fig. 6. The standard deviation of the wind speed and the wind direction were 1.7 m/s and 23.5°, respectively, indicating that the proposed regrouping algorithm met the requirements for a high-quality sea surface wind field retrieval.

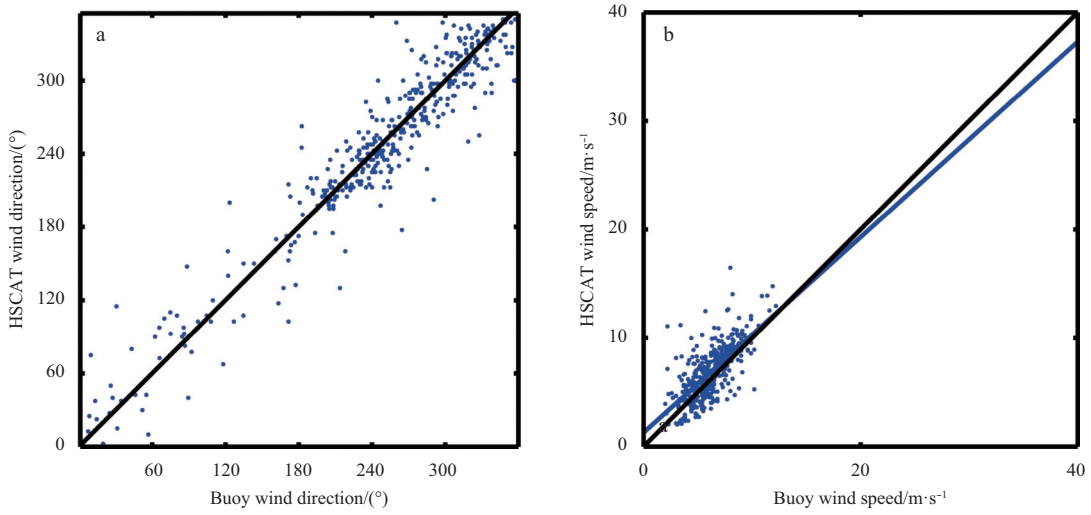

Fig. 6. Comparison of retrieved wind vectors from HSCAT and from buoy data.

5 Conclusions

In this study, we proposed a routine operational regrouping method for HSCAT data that maps time-ordered sigma0s and related parameters into a subtrack aligned grid of the WVCs. The regrouping method consisted of two critical steps: ground grid generation and sigma0 resampling. The HSCAT uses subtrack swath coordinates, in which the nadir track of the satellite is used as the center and the designated positions are specified in terms of a pair of along- and cross-track coordinates. To calculate the subtrack coordinates for the sigma0s, a "triangle marking" resampling method was applied by running a line that is perpendicular to the line of the nadir track through the center of a pulse's footprint. The three points, including the point of intersection, the center of the pulse's footprint, and the origin of the subtrack coordinate system, form a right triangle; the length of the two right-angled sides was used to represent the cross- and along-track coordinates in the subtrack coordinate system. To simplify the calculation, the position of the nadir point with the shortest distance to the intersection point was chosen to represent the position of the approximate intersection point. In addition, to ensure that the regrouping algorithm operates when positional data are missing for the nadir point position, a nadir point interpolation correction was implemented. To illustrate the capability of the proposed regrouping algorithm, we analyzed the distribution of the WVC positions and the wind vector retrieval results, which shows that the proposed regrouping algorithm satisfies the requirements for a high-quality sea surface wind field retrieval. Additionally, some distribution abnormalities were observed, such as cross-track blank strips in the regions where measurements were missing; however, these abnormalities were removed through the interpolation correction. To further validate the regrouping algorithm, a comparison between NDBC buoy wind data and the retrieved wind data was conducted and the results indicated that the proposed regrouping algorithm met the requirements for high-quality sea surface wind field retrieval.

References

Dunbar R S, Hsiao S V, Kim Y J. 2001. Science algorithm specification for SeaWinds on QuikSCAT and SeaWinds on ADEOS-II. Pasadena, California: Jet Propulsion Laboratory, 209–239

EUMETSAT. 2015. ASCAT Product Guide. EUM/OPS-EPS/MAN/04/0028, Eumetsat-Allee 1, D-64295 Darmstadt. Germany: EUMETSAT, 31

Lecomte P. 1998. ERS scatterometer instrument and the on-ground processing of its data. In: Proceedings of a Joint ESA-Eumetsat Workshop on Emerging Scatterometer Applications-From Research to Operations. The Netherlands: ESTEC

Naderi F M, Freilich M H, Long D G. 1991. Spaceborne radar measurement of wind velocity over the ocean-An overview of the NSCAT scatterometer system. Proceedings of the IEEE, 79(6): 850–866

Stoffelen A, de Vries J, Voorrips A. 2001. Towards the real-time use of QuikSCAT winds. Project Report. de Bilt, the Netherlands: KNMI

Verhoef A, Portabella M, Stoffelen A. 2012. High-resolution ASCAT scatterometer winds near the coast. IEEE Transactions on Geoscience and Remote Sensing, 50(7): 2481–2487

Vogelzang J. 2007. Two dimensional variational ambiguity removal (2DVAR). NWP SAF NWPSAF-KN-TR-004. http://www.eumetsat.int [2013-09-20/2015-01-01]

Vogelzang J, Stoffelen A, Verhoef A, et al. 2011. On the quality of high-resolution scatterometer winds. Journal of Geophysical Research, 116(C10): C10033, doi: 10.1029/2010JC006640

Zhang Yunhua, Jiang Jingshan, Zhang Xiangkun, et al. 2005. SZ-4 scatterometer mode of multimode microwave sensors (CNSCAT/M3RS). Remote Sensing Technology and Application (in Chinese), 20(1): 58–63

Zou Juhong, Xie Xuetong, Zhang Yi, et al. 2014. Wind retrieval processing for HY-2A microwave scatterometer. In: 2014 IEEE International Geoscience and Remote Sensing Symposium (IGARSS). Quebec City, QC: IEEE, 5160–5163